MATHEMATICAL BIOSCIENCES
AND ENGINEERING
Volume **14**, Number **3**, June **2017**

doi:10.3934/mbe.2017037

pp. **655–671**

GERMINAL CENTER DYNAMICS DURING ACUTE AND CHRONIC INFECTION

Samantha Erwin and Stanca M. Ciupe*

460 McBryde Hall
Virginia Tech
Blacksburg, VA 24061, USA

(Communicated by David M. Bortz)

Abstract. The ability of the immune system to clear pathogens is limited during chronic virus infections where potent long-lived plasma and memory B-cells are produced only after germinal center B-cells undergo many rounds of somatic hypermutations. In this paper, we investigate the mechanisms of germinal center B-cell formation by developing mathematical models for the dynamics of B-cell somatic hypermutations. We use the models to determine how B-cell selection and competition for T follicular helper cells and antigen influences the size and composition of germinal centers in acute and chronic infections. We predict that the T follicular helper cells are a limiting resource in driving large numbers of somatic hypermutations and present possible mechanisms that can revert this limitation in the presence of non-mutating and mutating antigen.

1. **Introduction.** The production of high-affinity antibodies capable of broad neutralization, viral inactivation, and protection against viral infections or disease requires activation, expansion, and maturation of B-cells into virus specific long-lived plasma and memory cells [46]. Germinal centers (GC) are the anatomical structures in which B-cells undergo somatic hypermutation, immunoglobulin class switching, and antigen-specific selection [30]. Somatic hypermutations are random and, therefore, the emergence of non-autoreactive, high-affinity B-cell clones requires strong selection through competition for survival signals [48]. The exact nature of these survival signals is poorly understood. T follicular helper (Tfh) cells have been identified as an important factor in driving B-cell hypermutation inside germinal centers [45]. Indeed, recent experiments have identified correlations between the density, function, and infection status of Tfh cells and the development of mature germinal centers [18, 31, 32, 33, 44, 43, 36].

Determining the characteristics of germinal centers such as their formation, size, and composition is important in understanding the protective mechanisms against pathogens that induce chronic infections. During HIV infections, only approximately 15-20% of chronically infected subjects develop antibodies with neutralization breadth [25, 40]. These antibodies are highly mutated compared to antibodies

2010 *Mathematics Subject Classification.* 92, 34.

Key words and phrases. B cells, Tfh cells, germinal centers, somatic hypermutations, and mathematical models.

* Corresponding author: Stanca M. Ciupe.

induced by most viral infections *in vivo* [41] or through vaccination [26]. For example, the high-affinity human antibody VRC01, which neutralizes 90% of HIV-1, has 70-90 somatic mutations [47] compared to the natural 5-10 somatic mutations [14]. The mechanisms that allow for the production of protective antibodies in some patients but not others are still under investigation [15, 39, 7, 16, 3].

Mathematical models have been used in the past to investigate the mechanisms responsible for B-cell somatic hypermutations inside the germinal centers [10, 28, 22, 21, 6, 12, 19, 23, 1, 36, 34]. Early studies hypothesized that re-entry into new GCs of B-cells from previous GCs may explain the affinity maturation process [10, 28]. Others showed that affinity maturation requires cyclic transition of B-cells between the two anatomical structures of the germinal center: the dark and light zones [22, 21, 6, 12, 19, 23, 1]. The models that incorporate dark and light zones investigated the role of molecular mechanisms such as competition for Tfh cells [23, 36, 34], antigen on the surface of follicular dendritic cells [37], binding sites [12], and clonal competition [35] in facilitating movement between the two zones. Lastly, they investigated internal and external stimuli that lead to germinal center termination [20, 27, 1]. These studies have not considered the mechanisms behind the emergence of large number of B-cell somatic hypermutations inside germinal centers as seen in some HIV patients [47]. Nor did they present hypotheses behind the absence of broadly neutralizing antibodies in the majority of HIV patients. Understanding the mechanistic interactions inside GCs that lead to production of plasma cells capable of producing antibodies with neutralization breadth forms the focus of this paper.

To address this, we develop mathematical models of germinal center formation that investigate the role of B-cell competition, Tfh cells, and antigen in inducing large numbers of B-cell somatic hypermutations, as seen in the few HIV patients that produce broadly neutralizing antibodies. We first develop a deterministic model of Tfh cell-B cell interactions to determine how B-cell selection and competition influences GC formation in acute infections. We fit the model to published germinal center B-cell data to estimate parameters. We then investigate the mechanisms that allow for emergence of highly mutated B-cell clones that are capable of protecting against chronic infections with non-mutating antigen, i.e. substances that do not mutate but stimulate antibody generation. Finally, we investigate how our predictions change when we consider antigenic mutation.

For a non-mutating pathogen, we predict that when only a few rounds of somatic hypermutations are needed for the clearance of a pathogen, as in acute infections, the Tfh cells are not limiting the emergence of high affinity B-cell clones. When large numbers of somatic hypermutations arise, however, a limitation in the number of Tfh cells may prevent B-cell clones of higher affinity from emerging and becoming the dominant B-cell population inside the germinal centers. Moreover, we predict that for a mutating pathogen which drives the somatic hypermutation of B-cells, emergence of B clones of highest affinity may be hindered not only through a limitation in the number of Tfh cells but also by the speed of the viral mutation.

2. Model of germinal center formation.

We develop a mathematical model of B-Tfh cell dynamics which considers the interaction between the naive CD4 T-cells (N), non-mutating antigen (V), pre-Tfh cells (H), Tfh cells (G), primed follicular B-cells (B_0), GC B-cells that have undergone i rounds of somatic hypermutations

(B_i), and plasma cells (P). Here $1 \leq i \leq n$ and n represents the maximum number of B-cell clones inside a single germinal center.

N cells are produced at rate s_N and die at per capita rate d_N and, upon encountering specific antigen V, migrate to the T:B cell border and become pre-Tfh cells H at rate α_N. H cells either migrate to GCs following interaction with primed follicular B-cells B_0 and differentiate into Tfh cells G at rate γ, or die at per capita rate d_H. G cells are lost through natural death at per capita rate d_G. Moreover, we assume that competition between B-cell clones B_i for Tfh cell-induced stimulation is limiting G population growth at rate η. This competition, in return, will limit the number of B-cells inside GCs and their transition between clones of higher affinity for the pathogen.

Primed follicular B-cells B_0 (B blasts) die at rate d and, upon interaction with pre-follicular helper cells H, move inside germinal centers where they undergo affinity maturation. We assume that each stage of affinity maturation requires Tfh cell help at the same rate σ and that each population B_i produces α offsprings B_{i+1}, for $1 \leq 1 \leq n-1$ [45]. B_is die at the same per capita rate d as B blasts. Lastly, cells in clone B_n leave germinal centers at rate κ to become plasma cells P capable of removing a non-mutating antigen V at rate μ.

The system describing these interactions is given by:

$$\frac{dN}{dt} = s_N - d_N N - \alpha_N V N, \tag{1a}$$

$$\frac{dH}{dt} = \alpha_N V N - d_H H - \gamma H B_0, \tag{1b}$$

$$\frac{dG}{dt} = \gamma H B_0 - d_G G - \eta G \sum_{i=1}^{n} B_i, \tag{1c}$$

$$\frac{dB_0}{dt} = -dB_0 - \sigma B_0 H, \tag{1d}$$

$$\frac{dB_1}{dt} = \alpha\sigma B_0 H - \sigma B_1 G - dB_1, \tag{1e}$$

$$\frac{dB_i}{dt} = \alpha\sigma B_{i-1} G - \sigma B_i G - dB_i, \tag{1f}$$

$$\frac{dB_n}{dt} = \alpha\sigma B_{n-1} G - dB_n - \kappa B_n, \tag{1g}$$

$$\frac{dP}{dt} = \kappa B_n, \tag{1h}$$

$$\frac{dV}{dt} = -\mu V P, \tag{1i}$$

for $1 \leq i \leq n-1$ with initial conditions $N(0) = s_N/d_N$, $B(0) = B_0$, $V(0) = V_0$ and all other populations are initially absent. Our goal is to determine the dynamical evolution of the total B-cell population in a single germinal center based on the availability of Tfh cells. We focus on the size and composition of B-cells in the germinal center,

$$B_t = \sum_{i=1}^{n} B_i, \tag{2}$$

for acute infections and for chronic infections where many rounds of affinity maturation lead to development of broadly neutralizing antibody-producing plasma cells, as seen in a few HIV infections [25, 40].

3. **Tfh-B-cell dynamics during acute infections.** In acute infections, B clones undergo between 5 and 10 steps of affinity maturation [14, 29, 27]. Without loss of generality, we set $n = 8$. We assume that $N(0) = 10^6$ naive CD4 T-cells per ml are recruited by the antigen V. Studies have shown that mature B-cell clones inside germinal centers are the progeny of as little as 3 precursor blasts [13, 11]. Therefore, the initial blast population is $B(0) = 3$ cells.

The B_t data was collected from young, pathogen free mice. The splenic germinal center B-cells' temporary responses to a T-dependent antigen were measured [9], therefore providing germinal center B-cell dynamics throughout an acute infection. The antigen V is the density of sheep red blood cells (sRBC) per ml injected into the mouse, $V(0) = 2 \times 10^8$ sRBC per ml. It elicits a B-cell expansion inside a germinal center and subsequent antigen clearance. Lastly, we assume that at the time of the infection, all the other populations are absent, *i.e.* $H(0) = G(0) = 0$ cells per ml and $P(0) = B_i(0) = 0$ cells, for $1 \leq i \leq n$.

In our model, the per capita death rates of all CD4 T-cells are equal, $d_N = d_H = d_G = 0.01$ per day [38], and the naive CD4 T-cell population is at equilibrium at the beginning of infection, *i.e.*, $s_N = d_N \times N_0 = 10^4$ cells per ml per day. Naive CD4 T-cells N are activated by antigen V at rate α_N and move to the follicles and become pre-Tfh cells H. Since the pre-follicular T-cell density is around 10^4 cells per ml and the ratio between G and H cells ranges between 2 and 4 in the first 10 days of germinal center formation [36], we adjust parameters $\alpha_N = 1.8 \times 10^{-11}$ ml per day per cell and $\gamma = 2$ per cell per day to reflect this fact.

B-cells in each B clone die at rate $d = 0.8$ per day [11], independent of affinity maturation class i. Since the dynamics of V and P do not affect the Tfh-B-cell interactions, we arbitrarily assign values for parameters $\kappa = 1.2$ per day and $\mu = 2$ per cell per day, the plasma cell production rate and antigen removal rate, respectively. We will later analyze the effect of varying these rates. A summary of initial conditions and fixed parameters is presented in Table 1.

We estimate the remaining parameters α, the B-cell offspring production rate, and σ, the B-cell transition rate, by fitting the total B_t population as given by (2), in the presence of competition for Tfh cell signaling, *i.e.* $\eta = 10^{-5}$ per cell per day, to published germinal center B-cell data [27, 9]. We used `nlinfit` in MATLAB R2014b (The MathWorks Inc., Natick, MA). The estimates and confidence intervals for α and σ are presented in Table 2.

3.1. **Numerical results.** The dynamics of all variables of system (1) over time for parameters in Tables 1 and 2 are shown in Figure 1. The number of offspring produced by each B-cell clone is $\alpha = 27.5$ and the transition rate is $\sigma = 1.1 \times 10^{-5}$ ml per cell per day. Competition for Tfh cell help does not affect the fit and B_t dynamics. Indeed, when η, the competition parameter, is decreased from 10^{-5} to 0 per cell per day and $\sigma = 1.1 \times 10^{-5}$ ml per cell per day the estimate for α, the B-cell offspring production rate, decreases by less than 1.5% to $\alpha = 27.1$. Therefore, we predict that the Tfh cell population is not inhibiting the emergence of B-cells that underwent the maximum 8 rounds of somatic hypermutation.

The total number of B-cells in the germinal center, B_t, reaches a maximum of 1147 cells, eleven days after infection and the germinal center dies out 29 days after infection (see Figure 1, panel a). Over time, the germinal center is formed by B-cell clones of the highest somatic hypermutation, with the maximum ratio between the peaks of two consecutive clones $B_i/B_{i-1} = 2.91$ occurring for $i = 5$. There is a delay between the peaks of each clone ranging between 0.3 and 2.1 days. For the

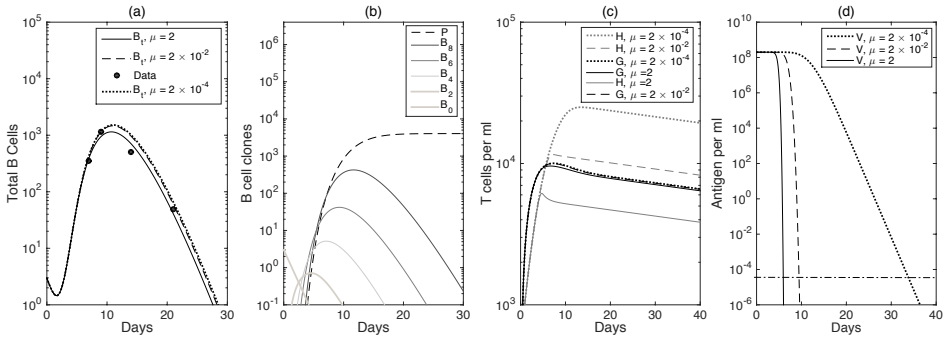

FIGURE 1. **Dynamics of model (2) applied to an acute infection.**(a) B_t as given by (2) versus data (•); (b) B-cells that underwent different levels of somatic hypermutations and plasma cells, for $\mu = 2$.; (c) Pre-Tfh cells H per ml and Tfh cells G per ml; and (d) Antigen per ml; for $\mu = 2$ per cell per day (solid lines), $\mu = 2 \times 10^{-2}$ per cell per day (dashed lines) and $\mu = 2 \times 10^{-4}$ per cell per day (dotted lines). The dashed-dotted line is the antigen limit of detection of 3×10^{-4} sRBC per ml. The other parameter values are given in Tables 1 and 2.

plasma cell production rate $\kappa = 1.2$ per day, plasma cells emerge 4.5 days following infection and reach a value of 4000 cells, 15 days following infection (see Figure 1, panel b).

The pre-Tfh and Tfh populations, H and G, reach their maximum density of 6.1×10^3 and 9.6×10^3 cells per ml, 5 and 7 days following infection, respectively. The $G : H$ ratio increases to 2.5, two days following infection and then levels off to 1.7 more Tfh than pre-Tfh cells (see Figure 1, panel c). A higher ratio, of as high as 4-times more Tfh than pre-Tfh cells, as predicted by [36], can be obtained if we increase γ, the pre-Tfh cell differentiation rate, by 50% (not shown). Once the antigen is eliminated, both H and G populations disappear.

For $\mu = 2$ per cell per day, the antigen is lost 5.9 days after infection. At that time V reaches 3×10^{-4} sRBC per ml (or 1 sRBC in the body). A reasonable concern is that varying this rate would affect the dynamics of the total B-cell population, as a prolonged antigenic stimuli would potentially lead to a larger germinal center that lasts for a longer period of time. To gain a deeper understanding of the role of μ, the antigen removal rate, in the B_t dynamics, we decrease μ by two and four orders of magnitude. As expected, when we decrease μ to 2×10^{-2} and 2×10^{-4} per cell per day, the time needed for the removal of antigen increases to 10 and 33 days following infection, respectively (see Figure 1, panel d). The maximum B_t increases by 28% and 32% respectively and germinal centers last for 30 days (see Figure 1, panel a). The μ effect on G population is not significant, but the H increases and exceeds the G population (see Figure 1, panel c).

3.2. **Sensitivity analysis.** We performed a focused analysis of the time-dependent sensitivity of model (1)'s trajectories to parameter variation, known as a semi-relative sensitivity analysis. We start by looking at the sensitivity of variables B_t and G to changes in the two fitted parameters α, the B-cell offspring production

rate, and σ, the B-cell transition rate, as follows. We define the absolute sensitivity variables $B_{t,q} = \frac{\partial B_t(t,q)}{\partial q}$ and $G_q = \frac{\partial G(t,q)}{\partial q}$. They are obtained by differentiating both sides of system (1) with respect to q, for $q = \{\alpha, \sigma\}$. The semi-relative sensitivity variables are calculated by multiplying the absolute sensitivity by the variables q.

In Figure 2 we compared the semi-relative sensitivity curves $qB_{t,q}$ and qG_q for $q = \sigma$ and $q = \alpha$. These parameters have complementary effects on both B_t and G populations. As such, if α, the B-cell offspring production rate, and σ, the B-cell transition rate, are doubled, B_t increases by a maximum of 6121.6 and 5166.6 cells at day 10 following infection (see Figure 2, top panel). Varying parameters α and σ has no effect on G for the first 5 days. After that time, their effect is negative. In particular, if either of the two parameters is doubled, then the G population decreases by 5366 or 5504 cells per ml at day 17 for σ and α respectfully (see Figure 2, bottom panel).

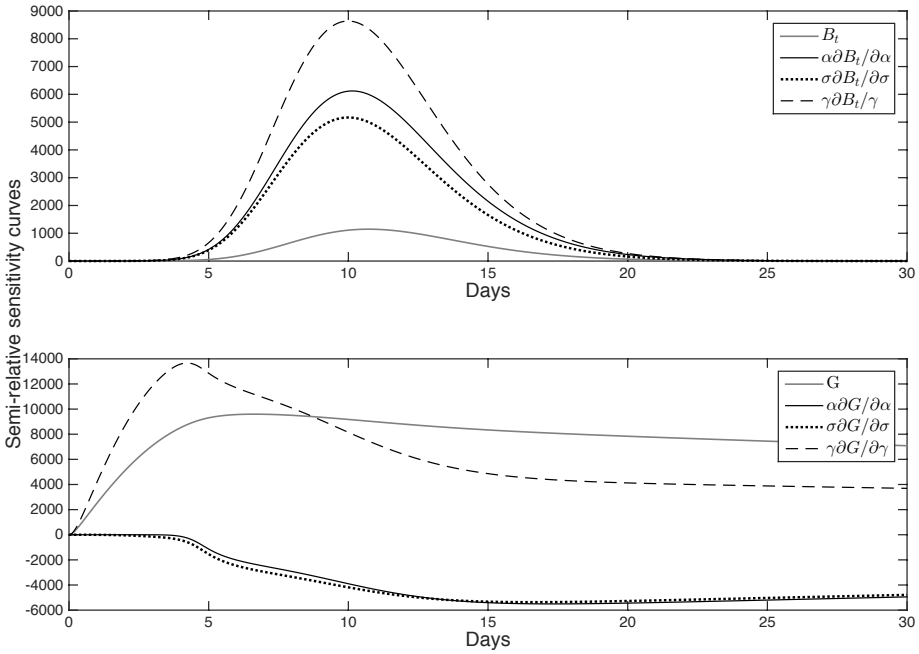

FIGURE 2. **Sensitivity Analysis.** B_t and G (grey lines) and the semi-relative sensitivity curves, $q\frac{\partial B_t}{\partial q}$ and $q\frac{\partial G}{\partial q}$, over time for $q = \alpha$ (solid lines), $q = \gamma$ (dotted lines) and $q = \sigma$ (dashed lines).

We further looked for parameters that have antagonistic effects on the G dynamics. We compared the semi-relative sensitivity curves $qB_{t,q}$ and qG_q for $q = \sigma$ and $q = \gamma$ (see Figure 2). These parameters have complementary effects on B_t (see Figure 2, top panel) and antagonistic effects on G (see Figure 2, bottom panel). In particular, while σ, the B-cell transition rate, has no effect on G four days following infection, doubling the value of γ, the pre-Tfh cell differentiation rate, leads to an increase in the G population by 1.37×10^4 cells per ml at day 4 (see Figure 2, bottom panel).

4. **Tfh-B-cell dynamics during chronic infections.** We next want to understand the size and B-cell clone compositions of germinal centers during prolonged antigenic stimuli. During chronic virus infections with viruses like HIV, the development of broadly neutralizing antibodies, with high mutation levels, can occur after many years of infection. For example, the high-affinity human antibody VRC01 has 70-90 mutations [47]. We will use model (1) and parameters in Tables 1 and 2 as a starting point for understanding how the B-cell and Tfh cell dynamics change when many rounds of somatic hypermutations are allowed. Most importantly, we want to determine the mechanistic interactions that allow for the emergence of a large enough B-clone with the highest level of mutation, which is capable of removing the antigen.

We represent highly mutated antibodies by increasing the level of admissible B-cell somatic hypermutations to $n = 50$ in model (1). We start by keeping all other parameters as in Tables 1 and 2. As expected, increasing n leads to an increase in the B_t population, with the B_t peak being two orders of magnitude higher and occurring two days earlier than in the $n = 8$ case. Such large germinal centers are not uncommon in persistent infections such as HIV [42], and subsequently we assumed the B-cell size to be reasonable and did not attempt to refit model (1) with $n = 50$ to the acute data. Under these assumptions, we predict that the germinal center terminates two days earlier, at 27 days following infection (see Figure 3, panel a).

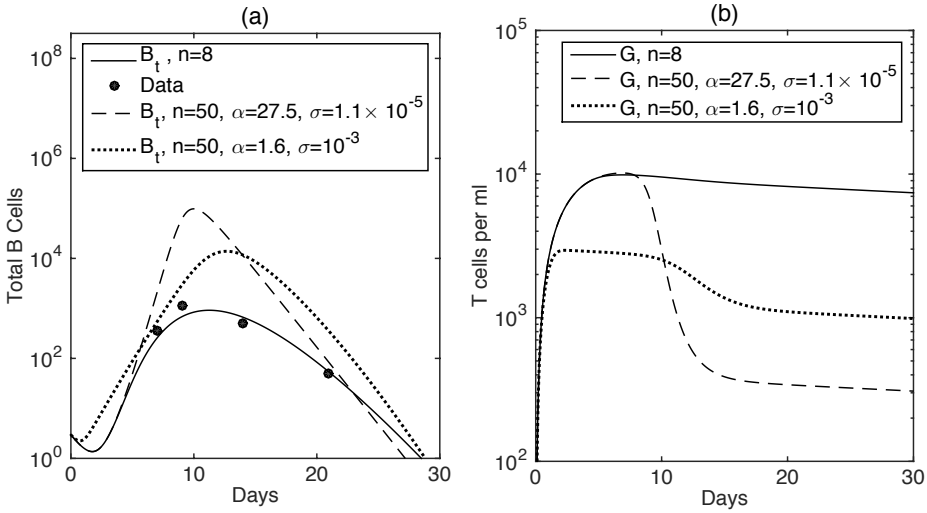

FIGURE 3. **Comparison of model (1)'s dynamics when n, α and σ are varied.** (a) B_t as given by (2) versus data (•); and (b) G per ml as given by model (1) for $n = 8$ (solid lines); $n = 50$, $\alpha = 27.5$, $\sigma = 1.1 \times 10^{-5}$ ml per cell per day (dashed lines); and $n = 50$, $\alpha = 1.6$, $\sigma = \times 10^{-3}$ ml per cell per day (dotted lines). The other parameters are given in Tables 1 and 2.

We observe that the Tfh cell population is smaller compared to the acute case during the contraction time, i.e. past 9 days following infection. This is due to competition between an increasing number of B-cell clones for Tfh cell stimuli as given by the term $\eta B_t G$ (see Figure 3, panel b).

To gain an understanding on the role of competition for Tfh cell help we compute and plot the distribution of B-cell clones for $n = 8$ and $n = 50$ at $t = 10$, $t = 20$, and $t = 30$ days after the germinal center initiation. For $n = 8$ and the three times considered, the late clones dominate the B_t population and, as time progresses, more and more of B_t is dominated by B_8, which is the clone that underwent the maximum rounds of hypermutations and the only clone giving rise to plasma cells (see Figure 4, top row). For $n = 50$, however, B_t is dominated by the clones that underwent $15 - 35$ rounds of somatic hypermutations at all times considered, and the B_{50} clone is never reached (see Figure 4, second row). Although there has been a slight movement to the later clones, there is very little change in the distribution between $t = 20$ and $t = 30$ days. Since only B_{50} produces plasma cells capable of removing virus, we predict that $dV/dt = 0$, and the virus remain at its initial value which was representative of a chronic infection.

Experimental data suggests that the key to developing therapies against chronic HIV infection lies in creating B-cells of the highest allowed level of somatic hypermutation [30]. Such later clones are instrumental for creating plasma and memory cells that produce highly mutated antibodies capable of neutralizing HIV virus. Our model is such that only the B-cells in the last clone become plasma cells that remove the virus, and since few B_{50} cells are being produced, the virus will persist. Therefore, we aim to understand what parameter changes will allow for the emergence of B-cell clones that underwent 50 rounds of affinity maturation, currently not observed in our predictions.

Not surprisingly, clone B_{50} can be achieved if the Tfh cells G are not a limiting value, in particular if we remove the competition term, *i.e.*, $\eta = 0$ per cell per day (see Figure 4, third row). Under this assumption, antigen V is eliminated 11.1 days following infection. In order to determine if additional interactions can lead to the same behavior, we keep $\eta = 10^{-5}$ per cell per day and adjust two different parameters. As such, if we increase 91-times the rate at which B-cell hypermutation is driven by interaction with Tfh cells, *i.e.* $\sigma = 0.001$ ml per cell per day, and we decrease 17.2-times the number of offspring produced during each clonal transition, *i.e.*, $\alpha = 1.6$ and keep the other parameters as in Tables 1 and 2, then the germinal center will contain the last clone B_{50} at all times. Moreover, B_{50} will become the dominant clone $t = 20$ days following infection (see Figure 4, bottom row). That means that decreasing the number of B-cells in each clone and speeding their transition rate into the next affinity class is sufficient in driving affinity maturation towards clones of the highest level of somatic hypermutation.

Under the adjusted values, $\alpha = 1.6$, the B-cell offspring production rate, and $\sigma = 10^{-3}$ ml per cell per day, the B-cell transition rate, the total germinal center B-cell population B_t peaks 13 days following infection and reaches a maximum of 1.39×10^4 cells, 12-times higher than in the acute case (see Figure 3, panel a). The Tfh population is 3.6-times smaller than in the acute and chronic cases for the first ten days, due to the decrease in offspring production. After day 10, the Tfh population decreases even further to 10^3 cells per ml (see Figure 3, panel b). However, this population is one order of magnitude higher than in the non-adjusted chronic case. This population is sufficient to provide help to all B-cell clones, such that the B_{50} clone can emerge, create plasma cells, and, most importantly, remove the antigen. For these adjusted parameters V is removed 9.5 days following infection.

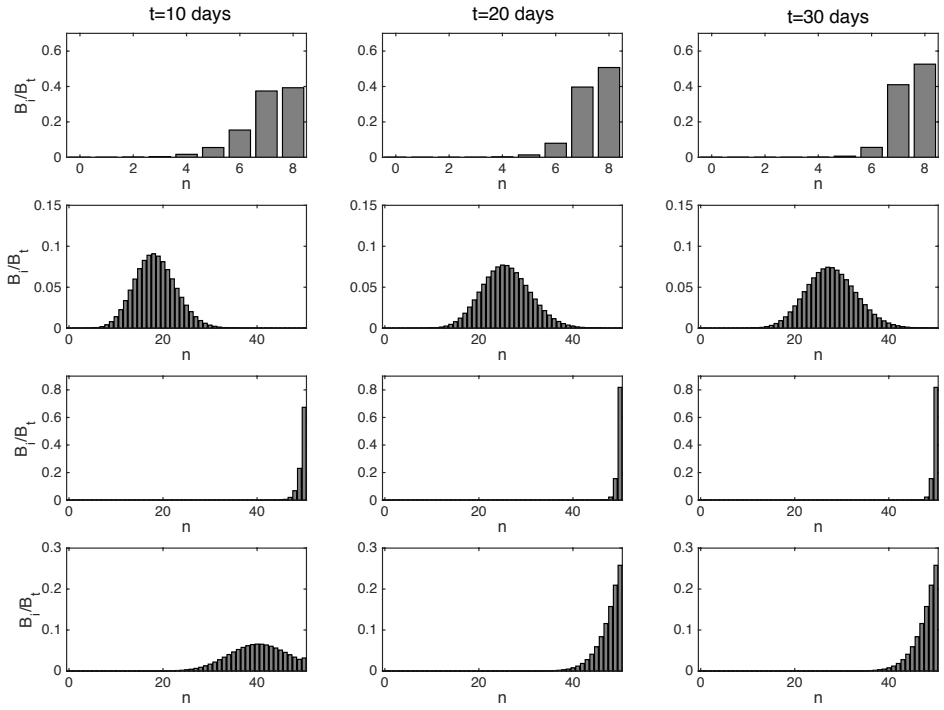

FIGURE 4. **B clone distribution in acute and chronic infections.** Clonal distribution B_i/B_t for $0 \le i \le n$, $t = 10$, $t = 20$, $t = 30$ days following infection for $n = 8$ (top row) and $n = 50$ (second row). Note that for $n = 8$ the germinal center contains the B clone with the highest level of somatic hypermutation B_8, while for $n = 50$ case the germinal center is dominated by middle clones and the B_{50} clone is absent. We then show two mechanisms to achieve the B_{50} clone: (third row) $\eta = 0$ and (bottom row) $\alpha = 1.6$, $\sigma = 10^{-3}$ ml per cell per day, $\eta = 10^{-5}$ per cell per day. B_t is given by (2), and the other parameters are given in Tables 1 and 2. In both situations clone B_{50} dominates the germinal center B-cell population 20 days following infection.

5. **Modeling mutating antigen.** Our model does not consider the effect of a mutating antigen, nor does it consider the need of both antigenic stimuli and Tfh cell help at each stage of B-cell somatic hypermutation. Previous studies predict that B-cell hypermutation is dependent on not only the ability of B-cells to recruit Tfh cell help, but also on the ability of the B-cells to retrieve and present antigen deposited on follicular dendritic cells [42, 4, 23, 34].

We extend model (1) to account for a mutating virus. In particular, we model a sequential mutation from virus V_0 to V_{n-1} at rate $0 < f < 1$. We only model the virus mutations that drive B-cell somatic hypermutations and all other mutations are ignored. Therefore, clone B_{i-1} is mutating into clone B_i due to stimuli from both Tfh cells and the respective virus variant V_{i-1} at rate $\sigma V_{i-1} G$, for $1 \le i \le n$. The T-cell populations, N, H and G are modeled as before with the addition that

total viral load, $V_t = \sum_{i=0}^{n-1} V_i$, can recruit pre-Tfh cells inside germinal centers to give rise to Tfh cells. As before, only the last clone, B_n, produces plasma cells, P. Under the assumption that broadly neutralizing antibody producing plasma cells are formed [42], P will remove all virus strains at rate μ. The modified model becomes

$$\frac{dV_0}{dt} = -fV_0 - \mu V_0 P, \tag{3a}$$

$$\frac{dV_i}{dt} = fV_{i-1} - fV_i - \mu V_i P, \tag{3b}$$

$$\frac{dV_{n-1}}{dt} = fV_{n-2} - \mu V_{n-1} P, \tag{3c}$$

$$\frac{dN}{dt} = s_N - d_N N - \alpha_N^{\phi} \sum_{i=0}^{n-1} V_i N, \tag{3d}$$

$$\frac{dH}{dt} = \alpha_N^{\phi} \sum_{i=0}^{n-1} V_i N - d_H H - \gamma H B_0, \tag{3e}$$

$$\frac{dG}{dt} = \gamma H B_0 - d_G G - \eta G \sum_{i=1}^{n} B_i, \tag{3f}$$

$$\frac{dB_0}{dt} = -d_0 B_0 - \sigma B_0 H V_0, \tag{3g}$$

$$\frac{dB_1}{dt} = \alpha\sigma B_0 H V_0 - \sigma V_1 B_1 G - dB_1, \tag{3h}$$

$$\frac{dB_j}{dt} = \alpha\sigma B_{j-1} G V_{j-1} - \sigma B_j V_j G - dB_j, \tag{3i}$$

$$\frac{dB_n}{dt} = \alpha\sigma B_{n-1} G V_{n-1} - dB_n - \kappa B_n, \tag{3j}$$

$$\frac{dP}{dt} = \kappa B_n, \tag{3k}$$

for $1 \leq i \leq n-2$ and $2 \leq j \leq n-1$. The initial conditions are $N(0) = s_N/d_N$, $B(0) = B_0$, $V(0) = V_0^{\phi}$ and all other populations are initially zero.

We numerically solve model (3), using parameters in Tables 1 and 2, $\alpha_N^{\phi} = 3.6 \times 10^{-6}$ ml per day per cell and $V_0^{\phi} = 10^3$ copies per ml (to account for an HIV-like antigen level). We vary mutation rate, f, to determine the effects of fast and slow mutating viruses on the GC's ability to produce broadly neutralizing antibodies and hence clear the virus. We compare the dynamics of B_t, V_t and G for $n = 8$ rounds of somatic hypermutation and varying mutation rates f. We see that fast viral mutation leads to the development of germinal centers containing large B_t populations. Indeed, for $f = 0.9$, germinal centers contain $B_t = 6.3 \times 10^4$ cells (see Figure 5, panel a, solid black lines). Moreover, fast mutation leads to fast production of clones with the highest degree of somatic hypermutation and consequently to plasma cell production (see Figure 5, panel a, solid grey line). As a result, virus is eliminated in the first two days after challenge (see Figure 5, panel c, solid line). For intermediate mutation rate, $f = 0.1$, the germinal center contains $B_t = 120$ cells (see Figure 5, panel a, dashed black line), plasma population is small and delayed (see Figure 5, panel a, grey dashed line), and, consequently, virus removal is delayed (see Figure 5, panel c, dashed line). Lastly, for slow mutation, $f = 0.01$, the germinal center contains $B_t = 55$ cells (see Figure 5, panel a, dotted

black line), plasma population is not produced at biological levels (cannot be seen in Figure 5, panel a) and, consequently, virus persists (see Figure 5, panel c, dotted line).

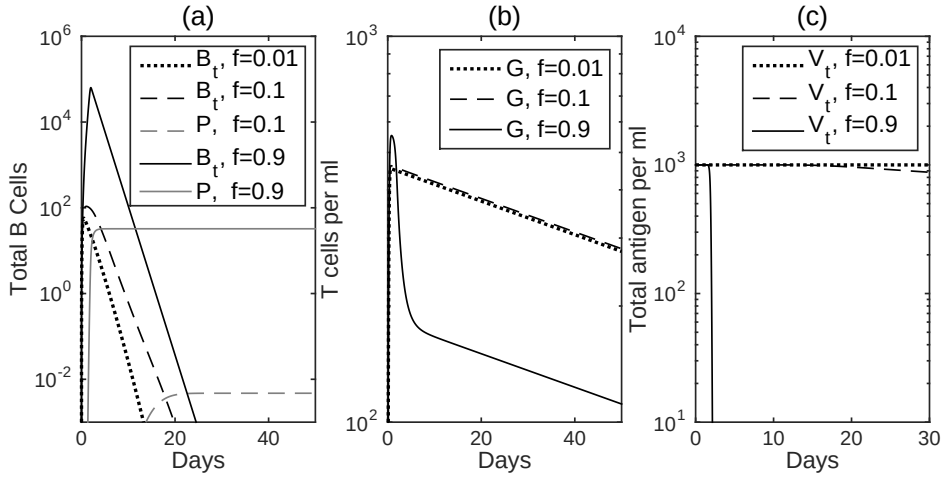

FIGURE 5. **Comparison of model (3)'s dynamics when f is varied.** (a) B_t and P, (b) G per ml, and (c) $V_t = \sum_{i=0}^{n-1} V_i$ as given by (3) for $n = 8$ and $f = 0.9$ (solid lines); $f = 0.1$ (dashed lines); $f = 0.01$ dotted lines. The other parameters are given in Tables 1, 2, $\alpha_N^\phi = 3.6 \times 10^{-6}$ and $V_0^\phi = 10^3$. Note that P for $f = 0.01$ is negligible.

We look in detail at the slow mutation case. For $f = 0.01$, B_8, the clone with the highest affinity maturation level, is not produced. That is due to the fact that virus strain V_7, which is needed for B_8 activation, increases above the limit of detection (of 50 copies per ml) only at 230 days after infection (see Figure 6, panel a, black line). By that time, the germinal center has been terminated (see Figure 6, panel b). This is due to faster clearance of B-cells through natural death compared to B-cell production in the presence of antigenic stimulation, *i.e.* $d >> \alpha\sigma V_{i-1}G$. Therefore, higher order B-cell clones and, consequently, plasma cells are not produced and virus will persist. This result is independent of the competition between B-cell clones for T follicular helper cell stimulation and is maintained even when $\eta = 0$. To produce later B-cell clones, antigen-independent B-cell proliferation is needed. Such proliferation will compensate for B-cell loss. A possible form for the B_j population is:

$$\frac{dB_j}{dt} = \alpha\sigma B_{j-1} G V_{j-1} - \sigma B_j V_j G + rB_j - dB_j, \tag{4}$$

where $1 \leq j \leq n$ and r is the per capita B-cell growth rate. If the antigen-independent proliferation rate is high enough, *i.e.* $r = 0.75 < d$ or $r = 0.8 = d$ per day, model (3) with adjusted equations (4) predicts plasma cell production for $n = 8$ and $f = 0.01$ (see Figure 7, panel c, dashed and dotted lines).

Lastly, when we consider that the number of somatic hypermutations needed to produce plasma cells is $n = 50$ (as in HIV patients that produce broadly neutralizing antibody [25, 40]), plasma cell production requires both the antigen-independent B-cell proliferation given by (4) and lack of competition between B-cell clones for Tfh

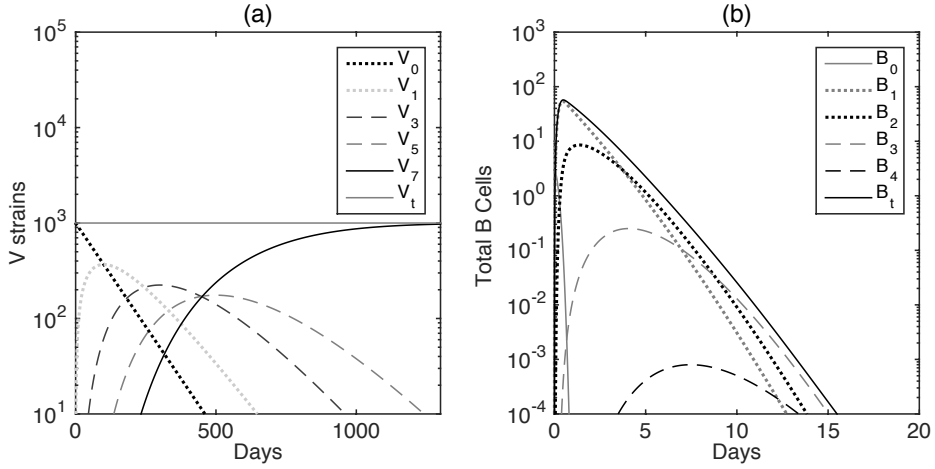

FIGURE 6. **Virus strains and B clone dynamics for slow mutating virus.** (a) V_i per ml, (b) B_i as given by (3) for $n = 8$ and $f = 0.01$. The other parameters are given in Tables 1, 2, $\alpha_N^\phi = 3.6 \times 10^{-6}$ and $V_0^\phi = 10^3$.

cell stimuli, *i.e.*, $\eta = 0$, for all $0.1 \leq f \leq 0.9$ (see Figure 7, panel c, dashed-dotted line).

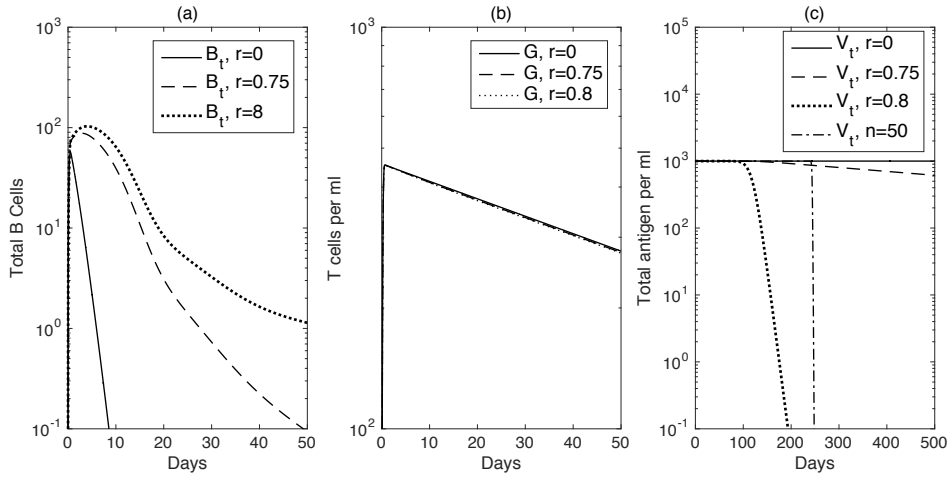

FIGURE 7. **Models (3)-(4)'s dynamics.** (a) B_t, (b) G per ml, and (c) $V_t = \sum_{i=0}^{n-1} V_i$ as given by (3) and (4) for $n = 8$, $f = 0.01$ and $r = 0$ (solid lines); $r = 0.75$ (dashed lines); and $r = 0.8$ (dotted lines); for $n = 50$, $f = 0.1$ and $r = 0.75$ (dashed-dotted line). The other parameters are given in Tables 1, 2, $\alpha_N^\phi = 3.6 \times 10^{-6}$ and $V_0^\phi = 10^3$.

6. **Discussion.** We developed a mathematical model of germinal center formation that includes competition between B-cell clones for Tfh cell stimulation. When we model responses to an acute pathogen requiring eight rounds of somatic hypermutations, the model reproduces the dynamics observed during germinal center formation, such as the size of the B-cell population, the time of germinal center termination, and the ratio between pre-Tfh and Tfh populations following antigenic challenge. We fit the model to data, and found that there are enough Tfh cells to allow for B-cell clones of the highest level of somatic hypermutations to emerge.

We then extended our model to allow for as many as 50-rounds of somatic hypermutations which are needed to fight chronic infections such as HIV. By expanding the model to chronic infections we aimed to determine the possible mechanisms that regulate or limit germinal center dynamics during persistent disease. Our study predicts that, under the acute B_t and Tfh parameter values, B clones that undergo 50 rounds of somatic hypermutation cannot emerge, and the germinal center B-cell population is composed of cells that underwent a maximum of 35-rounds of somatic hypermutations. This is due to loss of specific Tfh cells due to interaction with an increasing number of B-cell clones. This effect can be reversed and B-cell protection can be achieved either through removal of competition between the B-cell clones or through emergence of smaller size clones that mutate at a faster pace.

When modeling a mutating antigen that drives the rate of B-cell somatic hypermutations, plasma cell production is dependent on the speed of viral mutation. For eight rounds of somatic hypermutations, fast and intermediate mutating plasma cells capable of removing the virus are always produced. A slow mutating virus, however, requires an additional antigen-independent B-cell expansion that maintains enough B-cells inside germinal centers to induce the next round of somatic hypermutation even when the antigenic stimulus is delayed. As in the non-mutating case Tfh are not limiting the emergence of all B-cell clones. For 50-rounds of somatic hypermutation, however, competition among the B-cell clones for Tfh cell stimuli prevents the emergence of plasma cell production regardless of the speed of virus mutation. In this case, both antigen-independent B-cell proliferation and the removal of competition for Tfh stimuli between the B-cell clones, as in the non-mutating case are needed for plasma cells to emerge.

Our models assume that the B-cell division rate is exponentially distributed (as in [2]), and disregarded the inherent cell cycle delay shown experimentally and considered in previous modeling studies [24, 5, 17]. One of the reasons for this assumption is the fact that the B_0 population represents primed pre-follicular B-cells, rather than naive B-cells. These cells take less than two days to transition into the B_1 class (given our parameters and model assumptions). This is consistent with the observation in [8], which states that the first B-cell division occurred at 48 h. If a delayed model is considered, where the $\alpha\sigma B_{i-1}G$ terms are replaced by $f(t)\alpha\sigma B_{i-1}G$ with

$$f(t) = \begin{cases} 0, & t < \tau, \\ 1, & t \geq \tau, \end{cases} \tag{5}$$

and $\tau = 2$ days as in [8], than the results of model (1) presented in Figures 1, 3 and 4 are preserved with limited change in the parameter values (not shown).

Our work assumes that B-cells must undergo a strict number of mutations before maturing into plasma cells. We found that modeling the breadth of the response, through creating plasma cells of different affinities at each stage of B-cell somatic hypermutations did not change our results. Further work is needed to determine

the tradeoff between the need of high mutation numbers and the breadth of the immune response in fighting chronic infections.

In summary, we have developed models of Tfh-B-cell interactions to examine the dynamics of germinal centers in both acute and chronic infections. We found that T follicular helper cells are a limiting factor in the emergence of extremely high rounds of B-cell somatic hypermutations for both non-mutating and mutating virus. Moreover, we found that this limitation can be removed by inducing faster transition between clones and limiting the sizes of individual clones. Lastly, for a mutating virus that drives the somatic hypermutations, additional factors such as antigen-independent B-cell proliferation may be needed for plasma cell production and virus neutralization. These results may provide insight into the germinal center role during chronic infections.

Acknowledgments. We would like to thank the anonymous reviewers for the valuable comments and suggestions.

Name	Units	Value	Description	Confidence Intervals
α		27.469	B-cell offspring production rate	[14.015 40.924]
σ	ml per cell per day	1.1×10^{-5}	Affinity maturation rate	[4.8×10^{-6} 1.7×10^{-5}]

TABLE 2. Parameter estimates and confidence intervals.

REFERENCES

[1] C. Allen, T. Okada and J. Cyster, Germinal-center organization and cellular dynamcs, *Immunity*, **27** (2007), 190–202.
[2] B. Asquith, C. Debacq, A. Florins, N. Gillet, T. Sanchez-Alcaraz, A. Mosley and L. Willems, Quantifying lymphocyte kinetics in vivo using carboxyfluorescein diacetate succinimidyl ester (CFSE), *Proc Biol Sci*, **273** (2006), 1165–1171.
[3] D. Burton and J. Mascola, Antibody responses to envelope glycoproteins in HIV-1 infection, *Nat Immunol*, **16** (2015), 571–576.
[4] R. Cubas, J. Mudd, A. Savoye, M. Perreau, J. van Grevenynghe and et al, Inadequate T follicular cell help impairs B cell immunity during HIV infection, *Nat Med*, **19** (2013), 494–499.
[5] R. De Boer and A. Perelson, Quantifying T lymphocyte turnover, *J Theor Biol*, **327** (2013), 45–87.
[6] A. Hauser, M. Shlomchik and A. Haberman, In vivo imaging studies shed light on germinal-centre development, *Nat Rev Immunol*, **7** (2007), 499–504.
[7] B. Haynes, New approaches to HIV vaccine development, *Curr Opin Immunol*, **35** (2015), 39–47.
[8] P. Hodgkin, J. Lee and A. Lyons, B cell differentiation and isotype switching is related to division cycle number, *J Exp Med*, **184** (1996), 277–281.
[9] K. Hollowood and J. Macartney, Cell kinetics of the germinal center reaction - a stathmokinetic study, *Eur J Immunol*, **22** (1992), 261–266.
[10] T. Kepler and A. Perelson, Cyclic re-entry of germinal center B cells and the efficiency of affinity maturations, *Immunol Today*, **14** (1993), 412–415.
[11] C. Kesmir and R. De Boer, A mathematical model on germinal center kinetics and termination, *J Immunol*, **163** (1999), 2463–2469.
[12] C. Kesmir and R. de Boer, A spatial model of germinal center reactions: Cellular adhesion based sorting of B cells results in efficient affinity maturation, *J Theor Biol*, **222** (2003), 9–22.
[13] F. Kroese, A. Wubbena, H. Seijen and P. Nieuwenhuis, Germinal centers develop oligoclonally, *Eur J Immunol*, **17** (1987), 1069–1072.

7. **Tables.**

Name	Value	Units	Description	Citation
s_N	10^4	cells per ml per day	Naive CD4 T-cell recruitment rate	[38]
d_N	0.01	per day	Naive CD4 T-cell death rate	[38]
α_N	1.8×10^{-11}	ml per day per cell	Pre-Tfh cell production rate	
d_H	0.01	per day	Pre-Tfh cell death rate	[38]
d_G	0.01	per day	Tfh cell death rate	[38]
d	0.8	per day	B-cell death rate	[11]
κ	1.2	per day	Plasma cells production rate	
γ	2	per cell per day	Pre-Tfh cell differentiation rate	[36]
μ	2	per cell per day	Antigen removal rate	
η	10^{-5}	per cell per day	Tfh competition rate	
$N(0)$	10^6	cells per ml	Initial amount of CD4 T cells	[38]
$H(0)$	0	cells per ml	Initial amount of Pre-Tfh cells	
$G(0)$	0	cells per ml	Initial amount of Tfh cells	
$B_0(0)$	3	cells	Initial amount of B-cells	[13, 11]
$B_i(0)$	0	cells	Initial amount of B-cell clones	
$P(0)$	0	cells	Initial amount of plasma cells	
$V(0)$	2×10^8	per ml	Initial amount of non-mutating antigen	[9]

TABLE 1. Variables and fixed parameter values.

[14] R. Kuppers, M. Zhao, M. Hansmann and K. Rajewsky, Tracing B cell development in human germinal centers by molecular analysis of single cells picked from histological sections, *Embo J*, **12** (1993), 4955–4967.

[15] P. Kwong and J. Mascola, Human antibodies that neutralize HIV-1: Identification, structures, and B cell ontogenies, *Immunity*, **37** (2012), 412–425.

[16] V. L and M. Diaz, Autoreactivity in HIV-1 broadly neutralizing antibodies: Implications for their function and induction by vaccination, *Curr Opin HIV AIDS*, **9** (2014), 224–234.

[17] H. Lee, E. Hawkins, M. Zand, T. Mosmann, H. Wu and et al., Interpreting CFSE obtained division histories of B cells in vitro with Smith-Martin and cyton type models, *Bull Math Biol*, **71** (2009), 1649–1670.

[18] M. Lindqvist, J. van Lunzen, D. Soghoian, B. Kuhl, S. Ranasinghe and et all, Expansion of HIV-specific T follicular helper cells in chronic HIV infection, *J Clin Invest*, **122** (2012), 3271–3280.
[19] I. MacLennan, Germinal centers, *Annu Rev Immunol.*, **12** (1994), 117–139.
[20] M. Meyer-Hermann, E. Mohr, N. Pelletier, Y. Zhang, G. Victoria and K. Toellner, A theory of germinal center B cell selection, division, and exit, *Cell Reports*, **2** (2012), 162–174.
[21] M. Meyer-Hermann, M. Figge and K. Toellner, Germinal centres seen through the mathematical eye: B-cell models on the catwalk, *Trends in Immunol*, **30** (2009), 157–164.
[22] M. Meyer-Hermann and P. Maini, Cutting edge: Back to one-way germinal centers, *J Immunol*, **174** (2005), 2489–2493.
[23] M. Meyer-Hermann, P. Maini and D. Iber, An analysis of B cell selection mechanisms in germinal centers, *Math Med Biol*, **23** (2006), 255–277.
[24] H. Miao, X. Jin, A. Perelson and H. Wu, Evaluation of multitype mathematical models for CFSE-labeling experiment data, *Bull Math Biol*, **74** (2012), 300–326.
[25] I. Mikell, D. Sather, S. Kalams, M. Altfeld, G. Alter and L. Stamatatos, Characteristics of the earliest cross-neutralizing antibody response to HIV-1, *PLoS Pathog*, **7** (2011), 1–15.
[26] M. Moody, R. Zhang, E. Walter, C. Woods, G. Ginsburg and et al., H3N2 influenza infection elicits more cross-reactive and less clonally expanded anti-hemagglutinin antibodies than influenza vaccination, *PLoS One*, **6** (2011), e25797, 14pp.
[27] J. Moreira and J. Faro, Modelling two possible mechanisms for the regulation of the germinal center dynamics, *J Immunol*, **177** (2006), 3705–3710.
[28] M. Oprea and A. Perelson, Somatic mutation leads to efficient affinity maturation when centrocytes recycle back to centroblasts, *J Immunol*, **158** (1997), 5155–5162.
[29] M. Oprea, E. van Nimwegen and A. Perelson, Dynamics of one-pass germinal center models: Implications for affinity maturation, *Bull Math Biol*, **62** (2000), 121–153.
[30] S. Pallikkuth, A. Parmigiani and S. Pahwa, The role of interleukin-21 in HIV infection, *Cytokine growth factor rev*, **23** (2012), 173–180.
[31] M. Perreau, A.-L. Savoye, E. De Crignis, J. Corpataux, R. Cubas and et al, Follicular helper T cells serve as the major CD4 T cell compartment for HIV-1 infection, replication, and production, *J Exp Med*, **210** (2013), 143–156.
[32] J. Publicover, A. Gaggar, S. Nishimura, C. Van Horn, A. Goodsell and et al, Age-dependent hepatic lymphoid organization directs successful immunity to hepatitis B, *J Clin Invest*, **123** (2013), 3728–3739.
[33] J. Publicover, A. Goodsell, S. Nishimura, S. Vilarinho, Z. Wang and et al., IL-21 is pivotal in determining age-dependent effectiveness of immune responses in a mouse model of human hepatitis B, *J Clin Invest*, **121** (2011), 1154–1162.
[34] M. Radmacher, G. Kelsoe and T. Kepler, Predicted and inferred waiting times for key mutations in the germinal centre reaction: evidence for stochasticity in selection, *Immunol and Cell Bio*, **76** (1998), 373–381.
[35] T. Schwickert, G. Victoria, D. Fooksman, A. Kamphorst, M. Mugnier and et al, A dynamic T cell-limited checkpoint regulates affinity-dependent B cell entry into the germinal center, *J Exp Med*, **208** (2011), 1243–1252.
[36] Z. Shulman, A. Gitlin, S. Targ, M. Jankovic, G. Pasqual and et al., T follicular helper cell dynamics in germinal centers, *Science*, **341** (2013), 673–677.
[37] G. Siskind and B. Benacerraf, Cell selection by antigen in the immune response, *Adv. Immunol.*, **10** (1969), 1–50.
[38] M. Stafford, L. Corey, Y. Cao, E. Daar, D. Ho and A. Perelson, Modeling plasma virus concentration during primary HIV infection, *J theor Biol*, **203** (2000), 285–301.
[39] L. Stamatatos, HIV vaccine design: The neutralizing antibody conundrum, *Curr Opin Immunol*, **24** (2012), 316–323.
[40] L. Stamatatos, L. Morris, D. Burton and J. Mascola, Neutralizing antibodies generated during natural HIV-1 infection: Good news for an HIV-1 vaccine?, *Nat Med*, **15** (2009), 866–870.
[41] L. Verkoczy, G. Kelsoe, M. Moody and B. Haynes, Role of immune mechanisms in induction of HIV-1 broadly neutralizing antibodies, *Curr Opin Immunol*, **23** (2011), 383–390.
[42] G. Victora and L. Mesin, Clonal and cellular dynamics in germinal centers, *Curr Opin Immunol*, **28** (2014), 90–96.
[43] C. Vinuesa, HIV and T follicular helper cells: A dangerous relationship, *J Clin Invest*, **122** (2012), 3059–3062.

[44] C. Vinuesa, I. Sanz and M. Cook, Dysregulation of germinal centres in autoimmune disease, *Nat Rev Immunol*, **9** (2009), 845–857.
[45] J. Weinstein, S. Hernandez and J. Craft, T cells that promote B-cell maturation in systemic autoimmunity, *Immunol Rev*, **247** (2012), 160–171.
[46] I. Wollenberg, A. Agua-Doce, A. Hernandez, C. Almeida, V. Oliveira and et al., Regulation of the germinal center reaction by Foxp3+ follicular regulatory T cells, *J Immunol*, **187** (2011), 4553–4560.
[47] X. Wu, T. Zhou, J. Zhu, B. Zhang, I. Georgiev and et al., Focused evolution of HIV-1 neutralizing antibodies revealed by structures and deep sequencing, *Science*, **333** (2011), 1593–1602.
[48] X. Zhang, S. Ing, A. Fraser, M. Chen, O. Khan, J. Zakem and et al., Follicular helper T cells: New insights into mechanisms of autoimmune diseases, *Ochsner J*, **13** (2013), 131–139.

Received February 16, 2016; Accepted October 12, 2016.

E-mail address: sherwin@vt.edu
E-mail address: stanca@math.vt.edu